FLUCTUATION INTERACTIONS OF COLLOIDAL PARTICLES

T. Ocampo-Delgado[a], *B. Ivlev*[a,b*]

[a]*Instituto de Física,*
Universidad Autónoma de San Luis Potosí San Luis Potosí
San Luis Potosí 78000, Mexico

[b]*Department of Physics and Astronomy and NanoCenter,*
University of South Carolina
Columbia, South Carolina 29208, USA

For like-charged colloidal particles, two mechanisms of attraction between them survive when the interparticle distance is larger than the Debye screening length. One of them is the conventional van der Waals attraction and the second is the attraction mechanism mediated by thermal fluctuations of particle position. The latter is related to the effective variable mass (Euler mass) of the particles produced by the fluid motion. The strongest attraction potential (up to the value of the temperature T) corresponds to the case of uncharged particles and a relatively large Debye screening length. In this case, the third attraction mechanism is involved. It is mediated by thermal fluctuations of the fluid density.

1. INTRODUCTION AND AN OVERVIEW

Systems of charged colloidal particles exhibit a variety of unusual physical properties [1–3]. Colloidal particles can be arranged into crystals [4] and into structures with clusters and voids [5–7]. Colloidal systems may undergo different types of phase transition [8–13]. Topological phase transitions in a two-dimensional system of colloidal particles were discussed in [14, 15]. Unusual ensembles of colloidal particles were observed in Refs. [16–18]. In [19], buckling instabilities in confined colloidal crystals were analyzed. Interesting behaviors of colloidal particles in external fields were reported in [20]. In an electrolyte, colloidal particles acquire some surface charge, screened by counterions at the Debye length λ_D, which results in the repulsion potential of Derjaguin, Landau, Verwey, and Overbeek (DLVO) [1, 2]. The DLVO theory, as a result of solution of the linearized Poisson–Boltzmann equation, has been questioned in [21, 22]. The generalization of the DLVO interaction via a modification of counterion screening was reported in [23].

The long-range attraction of like-charged particles is a matter of challenge and controversy in colloidal science. Very schematically, the story of the long-range attraction is as follows.

Initially, the long-range attraction of colloidal particles on a micron scale was reported in Ref. [24]. The authors reconstructed a pair potential from the measured correlation functions of a large ensemble of colloidal particles.

The authors of Refs. [25–27] published even more surprising results, the attraction being extended over a distance of almost 4 μm. They used a laser technique releasing two particles and observing their behavior. But their measurements were actually misinterpreted. Only a macroscopic hydromechanical effect associated with specificity of measurements but not a microscopic attraction mechanism was observed [28].

For a high-concentration particle ensemble, Bechinger and his group showed that different types of the interparticle potential result in almost identical correlation functions [29, 30]. The conclusion was that the interaction potential should be drawn from experiments not with a large ensemble but with a pair of colloidal particles. Another difficulty is related to an uncertainty in the observed particle position caused by diffraction, which can result in errors in the calculated pair potential (see Ref. [31] and the references therein). To reduce the diffraction uncertainty, ultraviolet observations should be used. Therefore, the reliability of calculation of the pair potential based on statistical properties of large ensembles of particles is questionable.

*E-mail: ivlev@caprine.physics.sc.edu

Despite the lack of reliability of various experiments on determination of a microscopic attraction mechanism of like-charges, it is always intriguing whether they attract in reality. We consider the following microscopic mechanism of attraction of two colloidal particles or a particle and a wall.

1. The conventional van der Waals attraction u_{vdW} [32] mediated by electromagnetic fluctuations.

2. The attraction U_{com} mediated by thermal compression fluctuations of a fluid.

3. The attraction I associated with thermal fluctuations of particle positions in a fluid. It results from variable particle masses (Euler masses) depending on the distance between them. This mechanism and the term "Euler mass" were proposed in Ref. [33].

In the first mechanism, the energy of fluctuating electromagnetic waves depends on the distance between particles and therefore leads to a force.

The first and the second mechanisms are generic because electromagnetic waves are just substituted by hydrodynamic ones.

In the third mechanism, moving particles drag a part of the fluid. The mass of the involved fluid depends on the distance between the particles. There is a thermal drift of the particles into the region with a larger effective mass, which is analogous to classical mechanics. This can be interpreted as an effective interaction mediated by thermal fluctuations of particle positions in a fluid. Formation of the variable mass involves high-frequency fluctuations of the particles when dissipative hydrodynamic effects are not important [34]. This corresponds to Euler hydrodynamics and gives rise to the term "Euler mass". The formation of Euler mass resembles the equipartition law when the mean kinetic energy is $T/2$ regardless of the dissipation. This is because the mean kinetic energy is also determined by high frequencies.

There is a substantial difference among the above attraction mechanisms. The first and the third ones survive when the interparticle distance becomes larger than the Debye screening length. At this distance, the DLVO repulsion is very small and the above two mechanisms are the only interactions. The second mechanism works when Coulomb effects in the fluid are not pronounced. Specifically, the particles are not charged and the Debye screening length is larger than the interparticle distance. A relative role of I and u_{vdW} was also analyzed in Ref. [35].

The goal of this paper is to study the three attraction potentials for two particles and for one near a wall (walls).

2. VAN DER WAALS INTERACTION

The energy of a fluctuating electromagnetic field around two particles depends on the distance R between them and therefore results in an interaction force. It is called the van der Waals force [32]. This force is mainly determined by the typical wave length λ of the fluctuating electromagnetic field because we should have $\lambda \sim R$. The permittivity of the particle material $\varepsilon(\omega)$ depends on the typical frequency $\omega \sim c/R$. We consider relatively large interparticle distances,

$$\frac{c}{\omega_0} < R, \qquad (1)$$

where ω_0 corresponds to an absorption peak of $\varepsilon(\omega)$. For example, $\omega_0 \sim 10^{16} \text{ s}^{-1}$ for water, and estimate (1) becomes $100 \text{ Å} < R$.

At a finite temperature, the typical wave length of the fluctuating electromagnetic field is $\hbar c/T$. In what follows, the interparticle distance is not too large,

$$R < \frac{\hbar c}{T}, \qquad (2)$$

which is equivalent to $R < 7.4 \ \mu\text{m}$ at room temperature.

We consider a typical interparticle distance R of the order of one or two microns, which agrees with conditions (1) and (2). In the optical range of ω, the permittivity is determined by the refractive index and can be substituted by the dielectric constant ε for particles and the dielectric constant ε_0 for the surrounded medium. When the two dielectric constants are close to each other,

$$\frac{\varepsilon - \varepsilon_0}{\varepsilon_0} \ll 1, \qquad (3)$$

we can use the approach of pairwise summation to calculate the energy of electromagnetic fluctuations (the van der Waals interaction energy) [32, 36] as

$$u_{vdW}(R) = -\frac{23\hbar c(\varepsilon - \varepsilon_0)^2}{64\pi^3 \varepsilon_0^{5/2}} \int\limits_{V_1} d^3 r_1 \int\limits_{V_2} \frac{d^3 r_1}{|\mathbf{r}_1 - \mathbf{r}_2|^7}. \quad (4)$$

In Eq. (4), the integrations are taken over the volumes of the two bodies. For two identical spherical particles of the radius a and center-to-center distance R, the integration in Eq. (4) results in [32, 36]

$$u_{vdW}(R) = -\frac{23}{1920\pi} \frac{(\varepsilon - \varepsilon_0)^2}{\varepsilon_0^{5/2}} \frac{\hbar c}{R} \left[\frac{2a^2(20a^2 - 3R^2)}{(R^2 - 4a^2)^2} + \frac{2a^2}{R^2} + \ln\frac{R^2}{R^2 - 4a^2} \right]. \quad (5)$$

For a spherical particle near a flat infinite wall, Eq. (4) yields

$$u_{vdW}(h) = -\frac{23}{640\pi} \frac{(\varepsilon - \varepsilon_0)^2}{\varepsilon_0^{5/2}} \frac{\hbar c}{a} \int\limits_{-1}^{1} \frac{(1-z^2)\,dz}{(z+h/a)^4}, \quad (6)$$

where h is the center-to-wall distance.

In the region of visible light for water, $\varepsilon_0 \approx 1.77$, for the typically used polystyrene colloidal particles, $\varepsilon \approx 2.40$. Therefore, the parameter $(\varepsilon - \varepsilon_0)/\varepsilon_0 \approx 0.35$ can be considered relatively small and hence Eqs. (5) and (6) are reasonable approximations for the van der Waals interaction.

3. INTERACTION MEDIATED BY COMPRESSION FLUCTUATIONS OF THE FLUID

We suppose that two particles are totally fixed inside a hydrodynamic medium and serve only as obstacles to fluid motion. There is no macroscopic motion in the system and the only motion is caused by thermal fluctuations of the fluid velocity $\mathbf{v}(\mathbf{r}, t)$. In this case, the free energy of thermal fluctuations of the fluid $F(R)$ depends on the distance R between the particles. The function

$$U_{com}(R) = F(R) - F(\infty) \qquad (7)$$

is an interaction mediated by compression fluctuations of the fluid analogously to the conventional van der Waals interaction mediated by electromagnetic fluctuations.

To find the free energy of thermal fluctuations of the fluid, we can start with the linearized Navier–Stokes equation [34]

$$\rho\frac{\partial \mathbf{v}}{\partial t} = -\nabla p + \eta \nabla^2 \mathbf{v} + \left(\zeta + \frac{\eta}{3}\right)\nabla\,\mathrm{div}\,\mathbf{v}. \qquad (8)$$

There are two types of fluid motion, one of them is transverse diffusion and the second is longitudinal sound waves associated with density variations. The equilibrium free energy of transverse motions is determined by the Boltzmann distribution of their kinetic energies and is independent of the friction coefficient in the thermal limit. The free energy of transverse motions in the thermal limit depends on the total volume, but is independent of the relative positions of the bodies. Therefore, transverse fluctuations do not result in an interaction.

Quite an opposite situation occurs for longitudinal motions, when the total free energy is a sum of energies of different sound modes. The spectrum of sound

waves depends on the distance R between bodies due to hydrodynamic boundary conditions on body surfaces, and this results in an R-dependence of the free energy. Hence, the fluctuation interaction between bodies is mediated by hydrodynamic sound waves, like the conventional van der Waals interaction is mediated by fluctuations of electromagnetic ones. With $\mathbf{v} = \nabla\partial\phi/\partial t$, it follows from Eq. (8) that

$$\rho\frac{\partial^2 \phi}{\partial t^2} = -\delta p + \left(\zeta + \frac{4\eta}{3}\right)\frac{\partial}{\partial t}\nabla^2 \phi. \qquad (9)$$

From thermodynamic relations and the continuity equation, we can obtain $\delta p = -\rho s^2 \nabla^2 \phi$, where s is the adiabatic sound velocity [34]. At the typical frequency $\omega \sim s/a \sim 10^{11}$ s^{-1} (with $a \sim 1$ μm being the particle radius), the dissipative term in Eq. (9) is small and we can write

$$\frac{\partial^2 \phi}{\partial t^2} - s^2 \nabla^2 \phi = 0. \qquad (10)$$

According to the small-friction limit, the boundary condition for the normal derivative $\nabla_n \phi = 0$ to Eq. (10) corresponds to the Euler fluid [34]. From the general standpoint, the free energy of a system of harmonic oscillators is independent of friction in the thermal limit.

In an electrolyte, the dispersion law of sound waves can be approximated as

$$\omega^2(\mathbf{q}) = s^2 q^2 + \frac{s^2}{\lambda_D^2}, \qquad (11)$$

where λ_D is the Debye screening length. We first consider the case of two infinite parallel walls separated by a distance R. The free energy per unit area of the system is expressed as a sum of energies of independent oscillators according to general rules of statistical physics,

$$F = T \int \frac{d^2k}{(2\pi)^2} \sum_{n=1}^{\infty} \ln\left[\omega\left(\mathbf{k}, \frac{\pi n}{R}\right)\right]. \qquad (12)$$

Performing the same steps as in Ref. [33], we obtain the interaction mediated by compression fluctuations in the form

$$U_{com} = \frac{T}{32\pi R^2} \times$$

$$\times \int\limits_0^{\infty} dz \ln\left[1 - \exp\left(-\sqrt{z + \frac{4R^2}{\lambda_D^2}}\right)\right]. \qquad (13)$$

In the limit cases, Eq. (13) becomes

$$U_{com} = \begin{cases} -\zeta(3)/16\pi R^2, & R \ll \lambda_D, \\[2mm] -\dfrac{\exp(-2R/\lambda_D)}{8\pi R\lambda_D}, & \lambda_D \ll R, \end{cases} \qquad (14)$$

where $\zeta(3) \approx 1.202$ is the Riemann zeta function value. At a large R, the interaction in (14) is screened on the length $\lambda_D/2$. The possibility of an interaction mediated by nonelectromagnetic fluctuations was proposed in [32]. The first formula in (14) was obtained in Ref. [33]. It is similar to the result in Ref. [36] for electromagnetic fluctuations and perfectly conducting planes.

The fluctuation interaction in (13) depends on the Debye screening length. This is due to summation over all wave vectors in the free energy and results in its dependence on the density of states, which, in turn, depends on the form of the spectrum. In our case, the spectrum $\omega = s(k^2 + \lambda_D^{-2})^{1/2}$ introduces a λ_D-dependence in the free energy.

When two objects are not flat but are close enough and interact by small parts of their surfaces, which are almost flat, the interaction potential can be derived from flat approximation (14) by integrating over the surfaces. For example, for a particle close to a flat wall, in the case where the center-to-wall distance h is smaller than the particle radius a, the interaction can be calculated as in Ref. [33]:

$$U_{com} = -\frac{\zeta(3)}{8} T \frac{a}{h-a}, \quad h-a \ll a, \lambda_D. \quad (15)$$

The analogous result for two spheres with the center-to-center distance R is

$$U_{com} = -\frac{\zeta(3)}{16} T \frac{a}{R-2a}, \quad R-2a \ll a, \lambda_D. \quad (16)$$

Equations (15) and (16) hold in a nonelectrolytic fluid or in an electrolyte with a sufficiently large screening length.

4. WHICH MECHANISM SURVIVES IN AN ELECTROLYTE?

In an electrolyte, the interaction U_{com} mediated by plasmons is strongly screened (see (14)). The van der Waals interaction u_{vdW}, mediated by photons of visible-range frequencies, is not sensitive to the plasmon effects. The mechanism of variable mass is connected solely with incompressible fluid fluctuations. Therefore, only the conventional van der Waals interaction u_{vdW} and variable mass mechanisms I can survive in an electrolyte. The interaction due to variable mass is considered in the following sections.

5. VARIABLE MASS MECHANISM

To illustrate the variable mass mechanism, we consider a simple mechanical analogy. We suppose that a classical nondissipative particle of the total energy E moves in the harmonic potential αx^2. When the particle mass is constant, the mean displacement $\langle x \rangle = 0$ in the harmonic potential. But in the case of a variable mass $m(x)$, the mean displacement $\langle x \rangle \neq 0$. This is because the particle velocity is smaller in the region of a larger mass, just to keep the total energy constant. Accordingly, the particle spends more time in the region of larger mass. This is equivalent to a certain effective attraction $I(x)$ to the region of larger mass. As shown in Ref. [33], for a slowly varying $m(x)$, the total effective potential becomes $\alpha x^2 - (E/2) \ln m(x)$.

A real particle with friction participates in the Brownian motion characterized by a certain temperature T. We briefly repeat the main arguments leading to the effective potential I [33]. The Langevin equation describing such processes has the form

$$m(x)\ddot{x} + \frac{1}{2}\frac{\partial m}{\partial x}\dot{x}^2 + \frac{\partial V(x)}{\partial x} + \eta\dot{x} =$$
$$= \text{stochastic force.} \quad (17)$$

Short-time fluctuations of the velocity $\dot{x}$ are well separated from the slow drift in an effective potential. Indeed, according to the fluctuation–dissipation theorem, the mean value of the kinetic energy $\langle m\dot{x}^2/2 \rangle = T/2$ corresponds to the equipartition law and is essentially given by short-time fluctuations related to the infinitely large circle in the complex frequency plane. Substituting that mean value in Eq. (17) leads to the effective potential $V(x) + I(x)$ [33], where

$$I(x) = -\frac{T}{2}\ln m(x). \quad (18)$$

Expression (18) is an exact result in the thermal limit (no quantum fluctuations), as is the equipartition law.

We recall what happens in the conventional case of position-independent masses. In the thermal limit, we can then set all frequencies equal to zero because they provide only quantum corrections to the partition function. The remaining part of the partition function is determined solely by the potential energy and does not depend on velocities. The scenario changes for a position-dependent mass. In that case, the following general arguments can be used. The partition function Z, which is proportional to the phase volume $\Delta p \Delta x$, acquires an additional positional dependence $\Delta p \sim \sqrt{Tm(x)}$ following from the momentum channel even in the thermal limit [33]. The free energy

$(-T \ln Z)$ results in interaction potential (18) obtained by a rigorous derivation procedure.

In the multidimensional case, the kinetic energy is expressed in terms of the mass tensor $m_{ij}(\mathbf{R})$ as

$$K = \frac{1}{2}\, m_{ij}(\mathbf{R})\dot{R}_i\dot{R}_j, \quad \omega \to \infty. \qquad (19)$$

As shown in Ref. [33], the interaction due to variable mass is then given by

$$I(\mathbf{R}) = -\frac{T}{2} \ln\left[\det m(\mathbf{R})\right]. \qquad (20)$$

The potential in (20) has a fluctuation origin and is mediated by fast fluctuations of velocity. In terms of coordinates, when form (19) is diagonalized, $\det m$ becomes a product of principal values and interaction (20) is reduced to a sum of terms related to principal coordinates.

6. INTERACTION MEDIATED BY THERMAL FLUCTUATIONS OF PARTICLE VELOCITIES

Calculating the effective fluctuation potential for systems with a complicated dynamics requires finding the mass tensor in the high-frequency limit and inserting it in Eq. (20). When particles in a fluid perform an oscillatory motion with a high frequency, the fluid velocity obeys the Euler equation everywhere in the fluid except a thin layer close to the particle surfaces [34]. Hence, finding the mass tensor in Eqs. (19)–(20) requires solving the Euler equation with a zero boundary condition for the normal component of the fluid velocity. For this reason, the mass corresponding to the high-frequency limit of particle dynamics can be called the Euler mass. The effective particle masses depend on the fluid mass involved in the motion. The fluid mass depends on the interparticle distance, and therefore the effective particle masses also depend on that distance.

In the case of one particle of a radius a in a bulk fluid, the Euler mass tensor has the form [34]

$$m_{ij} = \frac{4\pi a^3}{3}\left(\rho_0 + \frac{\rho}{2}\right)\delta_{ij}, \qquad (21)$$

where ρ_0 is the mass density of the particle and ρ is the fluid density. The first term in Eq. (21) is related to the proper mass of the particles and the second is associated with the fluid motion.
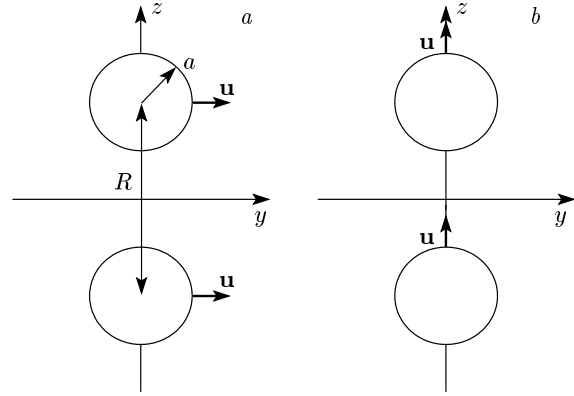

Fig. 1. Arrangements of particles with velocities u to calculate the mass M_x (a) and M_z (b) in Eq. (23)

6.1. Two particles in an infinite fluid

We now calculate the Euler mass tensor for two identical particles in a fluid. The fluid velocity normal to the particle surface should be equal to the normal particle velocity on its surface. If the particle velocities are $\mathbf{u}_1$ and $\mathbf{u}_2$, there are four independent quadratic combinations $\mathbf{u}_1^2 + \mathbf{u}_2^2$, $\mathbf{u}_1\mathbf{u}_2$, $(\mathbf{R}\cdot\mathbf{u}_1)(\mathbf{R}\cdot\mathbf{u}_2)$, and $[(\mathbf{R}\cdot\mathbf{u}_1)^2 + (\mathbf{R}\cdot\mathbf{u}_2)^2]$. We make the velocity transformation

$$\mathbf{V} = \frac{\mathbf{u}_1 + \mathbf{u}_2}{\sqrt{2}}, \quad \mathbf{v} = \frac{\mathbf{u}_1 - \mathbf{u}_2}{\sqrt{2}}. \qquad (22)$$

In terms of the new velocities, the kinetic energy can be written as

$$K = \frac{1}{2}\sum_{i=1}^{3}\left[M_i(\mathbf{R})V_i^2 + m_i(\mathbf{R})v_i^2\right], \qquad (23)$$

where $i = 1, 2, 3$ respectively correspond to x, y, z. Expression (23) involves only four independent masses because $M_x = M_y$ and $m_x = m_y$. The proper masses of the particles $4\pi a^3\rho_0/3$ can be separated from the fluid ones by writing

$$M_i = \frac{4\pi a^3}{3}\left[\rho_0 + \frac{\rho}{2}G_i\left(\frac{R}{a}\right)\right],$$

$$\qquad (24)$$

$$m_i = \frac{4\pi a^3}{3}\left[\rho_0 + \frac{\rho}{2}g_i\left(\frac{R}{a}\right)\right].$$

According to Eq. (21), $G(\infty) = g(\infty) = 1$.

The easiest way to calculate the masses is to use the method illustrated in Figs. 1 and 2, where the particle velocities are shown by arrows. The kinetic energy of the fluid in Figs. 1a and 1b is $(2\pi a^3/3)G_{x,z}(R/a)u^2$.
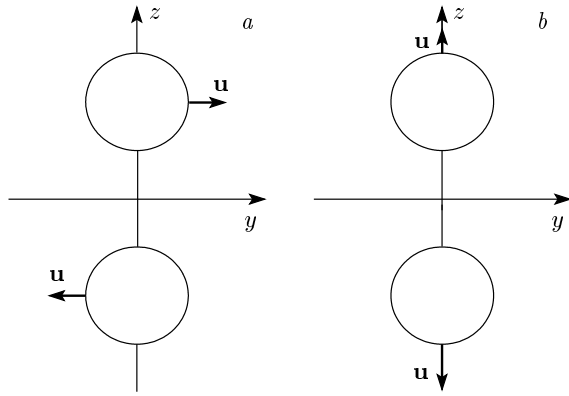
Fig. 2. Arrangements of particles with velocities u to calculate the mass m_x (*a*) and m_z (*b*) in Eq. (23)

Analogously, the fluid kinetic energy in Figs. 2*a* and 2*b* is $(2\pi a^3/3)g_{x,z}(R/a)u^2$. Interaction potential (20) becomes

$$I(R) = -T\left[\ln\frac{[2\rho_0+\rho G_x(R/a)][2\rho_0+\rho g_x(R/a)]}{(2\rho_0+\rho)^2} + \right.$$
$$\left. + \frac{1}{2}\ln\frac{[2\rho_0+\rho g_z(R/a)][2\rho_0+\rho G_z(R/a)]}{(2\rho_0+\rho)^2}\right]. \quad (25)$$

The function $I(R)$ tends to zero as $R \to \infty$.

6.2. One particle near an infinite wall

We consider one particle of a radius a placed in a half-space of the fluid filling the volume $z > 0$. The center-to-plane distance is h (the plane is at $z = 0$). The boundary condition at the particle surface is the equality of the normal components of the fluid and the particle velocities. The normal velocity component of the fluid velocity at the flat surface is zero. Obviously, the total kinetic energy is half that calculated in the previous subsection corresponding to Fig. 1*a* (the x and y components) and Fig. 2*b*, which are related to the zero normal velocity of the fluid at $z = 0$.

It is now easy to write the interaction potential using the results in the previous subsection. It is given by

$$I(h) = -T\left[\ln\frac{2\rho_0 + \rho G_x(2h/a)}{2\rho_0 + \rho} + \right.$$
$$\left. + \frac{1}{2}\ln\frac{2\rho_0 + \rho g_z(2h/a)}{2\rho_0 + \rho}\right], \quad (26)$$

where the functions G_x and g_z are the same as in the previous subsection.

6.3. One particle near two infinite perpendicular walls

This situation is shown in Figs. 3–5. The particle is placed in the fluid limited by the conditions $y < 0$ and $z > 0$. The other image particles, shown with dashed curves, are introduced in order to satisfy the boundary conditions on the planes $z = 0$ and $y = 0$ of zero normal velocities of the fluid. If we consider the whole space with the introduced image particles, the total kinetic energies are

$$K_i = 4\frac{4\pi a^3}{3}\left[\rho_0 + \rho f_i\left(\frac{h}{a},\frac{D}{a}\right)\right]\frac{u^2}{2} \quad (27)$$

with $i = 1, 2, 3$ for Figs. 3, 4, 5 respectively; the velocities of all particles are equal to u. Analogously to the previous cases, the interaction potential is

$$I(h, D) = -\frac{T}{2}\sum_{i=1}^{3}\ln\frac{2\rho_0 + \rho f_i(h/a, D/a)}{2\rho_0 + \rho}. \quad (28)$$

The boundary conditions are of the same type as in Sec. 6.1.

7. NUMERICAL METHOD TO CALCULATE THE INTERACTION POTENTIAL

In our case, the fluid velocity is $\mathbf{v} = \nabla\varphi$, where the potential φ satisfies the Laplace equation $\nabla^2\varphi = 0$ with the boundary conditions specified in Sec. 6,

$$\mathbf{n}(\mathbf{u} - \nabla\varphi)\big|_S = 0, \quad (29)$$

where S is the total surface that restricts the fluid. S includes borders of the particles (with velocities $\mathbf{u}$) and walls (with zero velocity). The unit vector $\mathbf{n}$ is perpendicular to the surfaces. The kinetic energy of the fluid is $\int d^3 r\, \rho\mathbf{v}^2/2$. Therefore, the total kinetic energy of the system can be written as

$$K = \sum_i\left(\frac{\rho_0}{2}\mathbf{u}_i^2 - \frac{\rho}{2}\int_{S_i} dS\,\varphi(\mathbf{r})\mathbf{n}_i\cdot\mathbf{u}_i\right), \quad (30)$$

where summation ranges over all particles with the areas S_i.

The numerical method proposed to calculate the Euler masses is based on an iteration procedure. In what follows, we discuss this method for two particles in an infinite fluid. The zero approximation is
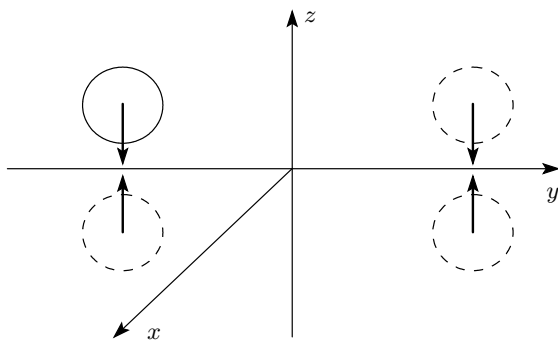
$$\varphi_0(\mathbf{r}) = \psi(\mathbf{r} - \mathbf{R}/2) + \psi(\mathbf{r} + \mathbf{R}/2), \quad (31)$$
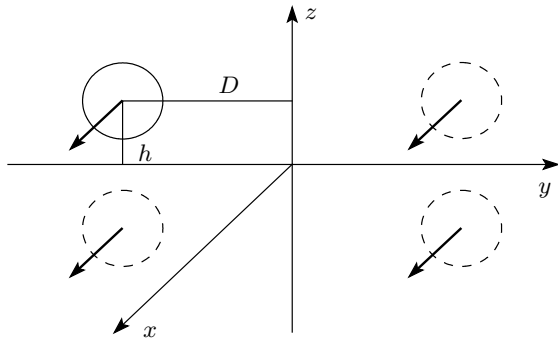
Fig. 3. A particle near two perpendicular walls. The three image particles, shown by the dashed curves, are added to consider the whole space with zero normal velocities of the fluid at the walls. This particle arrangement contributes to the function f_1 in Eq. (27)
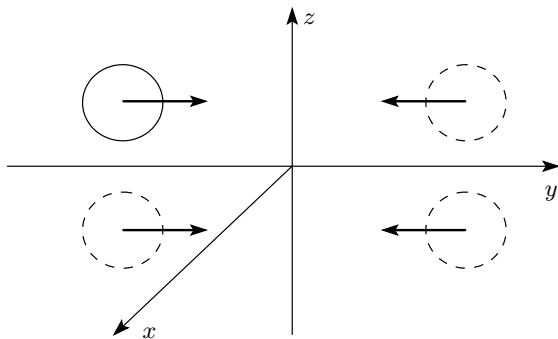
Fig. 4. The particle arrangement contributing to the function f_2 in Eq. (27)

Fig. 5. The particle arrangement contributing to the function f_3 in Eq. (27)

where the harmonic function ψ satisfies the equation

$$\psi(\mathbf{r}) = -\frac{1}{4\pi} \int dS' \, G(\mathbf{r}, \mathbf{r}') \, \mathbf{n}' \frac{\partial \psi(\mathbf{r}')}{\partial \mathbf{r}'} \qquad (32)$$

outside the sphere of the radius a centered at $\mathbf{r} = 0$. At the sphere surface, $\mathbf{n}\nabla\psi(\mathbf{r}) = u\cos\theta$ and θ is the

angle between $\mathbf{n}$ and $\mathbf{u}$. The integration in Eq. (32) is extended over the sphere surface, and the Green's function is given by

$$G(\mathbf{r}, \mathbf{r}') = \frac{2}{|\mathbf{r}-\mathbf{r}'|} + \frac{1}{a} \ln\left(\frac{r - r\cos\gamma}{|\mathbf{r}-\mathbf{r}'| + a - r\cos\gamma}\right), \quad (33)$$

where [37]

$$|\mathbf{r} - \mathbf{r}'| = \left(r^2 + a^2 - 2ar\cos\gamma\right)^{1/2},$$

$$\cos\gamma = \cos\theta\cos\theta' + \sin\theta\sin\theta'\cos(\phi - \phi').$$

The zeroth approximation potential $\varphi_0(\mathbf{r})$ in (31) provides the correct boundary conditions at the particle surfaces S in the limit $R \to \infty$. At a finite R, boundary condition (29) is not satisfied by the zeroth approximation (31), which therefore requires a modification. We can construct an iteration scheme $\varphi = \varphi_0 + \varphi_1 + \varphi_2 + \ldots$ by means of the recursion relation

$$\varphi_{n+1}(\mathbf{r}) = -\int\limits_{|\mathbf{r}'-\mathbf{R}/2|=a} \frac{dS'}{4\pi} G\left(\mathbf{r} - \frac{\mathbf{R}}{2}, \mathbf{r}' - \frac{\mathbf{R}}{2}\right) \times$$

$$\times \, \mathbf{n}' \cdot (\mathbf{u}\delta_{no} - \nabla\varphi_n(\mathbf{r}')) -$$

$$- \int\limits_{|\mathbf{r}'+\mathbf{R}/2|=a} \frac{dS'}{4\pi} G\left(\mathbf{r} + \frac{\mathbf{R}}{2}, \mathbf{r}' + \frac{\mathbf{R}}{2}\right) \times$$

$$\times \, \mathbf{n}' \cdot (\mathbf{u}\delta_{no} - \nabla\varphi_n(\mathbf{r}')), \quad (34)$$

where $n = 0, 1, 2, \ldots$ We have a fast convergence at large R because $\varphi_{n+1} \sim \varphi_n a/R$. At each iteration step, the boundary conditions becomes more and more exact with respect to the parameter a/R.

To calculate $G_x = G_y$ and G_z in Eq. (23) for Euler masses, we have to apply the scheme in (34) to the situations shown in Fig. 1a and Fig. 1b. Analogously, $g_x = g_y$ and g_z in Eq. (26) are associated with Fig. 2a and Fig. 2b.

From the functions G_x and g_z numerically found by the above method, we can also construct interaction (26) of a particle and a wall.

The same method is applicable to calculations of the potential in (28) for one particle near two perpendicular walls. Instead of two particles, we should then take four, with three of them playing the role of images (shown by dashed curves in Figs. 3–5). We do not describe an obvious modification of Eq. (32) in that case.

8. RESULTS

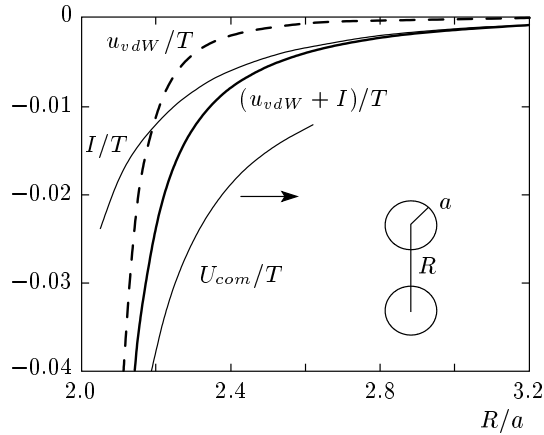In this section, we discuss the three different contributions to interaction of colloidal particles, listed in

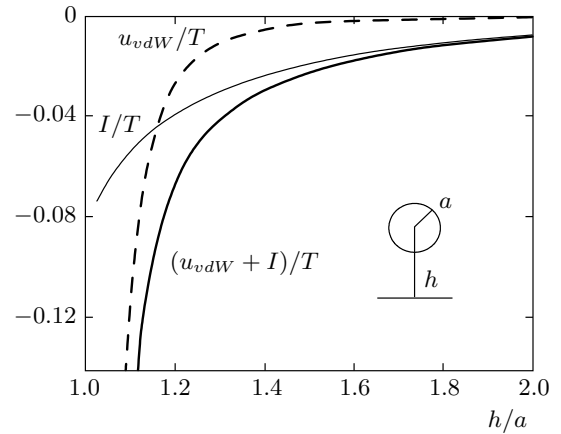**Fig. 6.** The numerically calculated attraction potentials for two particles in an infinite fluid; $\rho/\rho_0 = 1$

Fig. 7. The numerically calculated attraction potentials for one particle and an infinite flat wall; $\rho/\rho_0 = 1$

Fig. 8. The thick curve is the same as in Fig. 7. The thin curve represents interaction (15) mediated by thermal compression fluctuations of the fluid

Sec. 1, in various geometries: (i) two particles in a bulk fluid, (ii) one particle over a flat surface, and (iii) one particle near two perpendicular planes.

The interaction U_{com}, which is mediated by compression fluctuations of the fluid, plays the dominant role because it is relatively large, $U_{com}/T \sim (0.3\text{–}1.0)$, as follows from Figs. 6 and 8. On the other hand, the interaction U_{com} is strongly reduced by a finite Debye screening length λ_D. Therefore, this interaction can be observed in electrolytes with a large λ_D. In addition, surfaces of interacting objects should not be strongly charged to prevent the Coulomb repulsion from dominating over U_{com}.

In conventional electrolytes, normally used in experiments, only u_{vdW} (frequencies higher than the plasma frequency) and I (noncompressive fluctuations) survive on distances longer than λ_D, where the Coulomb repulsion of charged particles is screened.

Figure 6 relates to the case of two particles in a bulk fluid, Sec. 6.1. The interaction potential I (in the units of temperature T) is plotted by the thin solid curve. The conventional van der Waals interaction (5) is indicated by a dashed curve. The resulting potential is shown by a thick curve. It can be seen that U_{com} substantially exceeds the above interaction potentials.

Figures 7 and 8 correspond to the case of one particle near the wall, Sec. 6.2. As is clear from Fig. 8, U_{com} is not small and is of the order of T.

In Fig. 9, the potential I relates to one particle near two perpendicular walls.

When the intersurface distance is small, the potential I tends to a constant, whereas the van der Waals interaction is known to diverge. The results in Figs. 6–9 correspond to $\rho/\rho_0 = 1$. As this parameter increases,
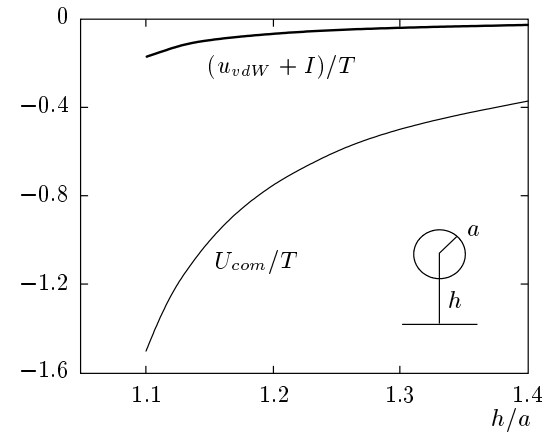
the attraction becomes more pronounced. For example, for $\rho/\rho_0 = 13.6$, related to colloidal particles in mercury, the attraction potential becomes more than two times larger in amplitude.
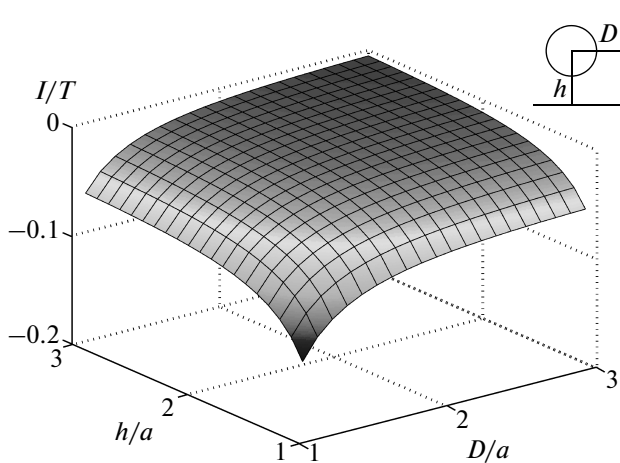
9. DISCUSSION

Is it possible to experimentally observe attraction of like-charged colloidal particles separated by a micron distance? We analyze different physical situations.

9.1. No Coulomb effects

The absense of Coulomb effects means that an electrolyte has a large Debye length λ_D and zero charges on

Fig. 9. The attractive interaction I in the units of T for one particle and two perpendicular walls; $\rho/\rho_0 = 1$

all surfaces. In this case, the DLVO repulsion is absent and the interaction mediated by compression fluctuations, U_{com}, substantially dominates the conventional van der Waals part u_{vdW} and the one mediated by particle velocities, I. As follows from Fig. 8, the interaction energy U_{com} of a particle of the radius 1 μm and a flat plane, at the surface-to-surface distance 0.15 μm, is $1T$. This attraction can be experimentally observed because it is relatively large.

9.2. Conventional particles in an electrolyte

For typical electrolytes and polystyrene particles [25], the DLVO repulsion has a short range and the interaction U_{com} is well suppressed. In this situation, only u_{vdW} and I survive. But the van der Waals interaction, u_{vdW} is weak and only I has chances to result in an observable attraction.

The peculiarity of the interaction I is that a particle is attracted stronger to a surface that geometrically adjusts its shape better. The flat surface in Fig. 7 adjusts the particle better than the counter-curved neighboring particle in Fig. 6. Also the geometry of two walls in Fig. 9 adjusts the particle shape better than one wall in Fig. 7. The attraction of a particle to a surface of the same type of curvature is the strongest.

The feature of the interaction I is that it is of the order of $0.05T$ (a particle near a flat wall) and of the order of $0.1T$ (a particle near two perpendicular walls) when the intersurface distance is of the order of $0.2a \sim 2000$ Å. At longer intersurface distances, the attraction I exceeds the van der Waals part.

It is promising to take a surface that adjusts the spherical particle better than two perpendicular planes. For example, it can be a cylinder with a particle inside. In this case, the interaction is a few or even ten times larger than $0.1T$ (two perpendicular planes). The minimum value of the interaction potential $0.1T$, where T is room temperature, is approximately a border of experimental resolution. Therefore, in a conventional electrolyte, the attraction of a micron-size particle to two perpendicular planes or to an interior surface of a cylinder can be observed experimentally.

REFERENCES

1. B. V. Derjaguin, *Theory of Stability of Colloids and Thin Films*, Consultans Bureau, New York (1989).

2. J. Israelachvili, *Intermolecular and Surface Forces*, Academic, San Diego, CA (1991).

3. P. C. Heimenz and R. Rajagopalan, *Principles of Colloidal and Surface Chemistry*, Dekker, New York (1997).

4. P. Pieranski, Phys. Rev. Lett. **45**, 569 (1980).

5. G. Y. Onoda, Phys. Rev. Lett. **55**, 226 (1985).

6. K. Ito, H. Yoshida, and N. Ise, Science **263**, 66 (1994).

7. S. J. Mejia-Rosales, R. Gamez-Gomez, B. I. Ivlev, and J. Ruiz-Garcia, Physica A **276**, 30 (2000).

8. P. M. Chaikin, P. Pincus, S. Alexander, and D. Hone, J. Colloid Interface Sci. **89**, 555 (1982).

9. Y. Monovoukas and A. P. Gast, J. Colloid Interface Sci. **128**, 533 (1989).

10. A. E. Larsen and D. G. Grier, Phys. Rev. Lett. **76**, 3862 (1996).

11. L. Radzihovsky, E. Frey, and D. Nelson, Bull. Amer. Phys. Soc. **45**, 698 (2000).

12. K.-H. Lin, J. C. Crocker, and A. G. Yodh, Bull. Amer. Phys. Soc. **45**, 698 (2000).

13. C.-H. Sow, C. A. Murray, R. W. Zehner, and T. S. Sullivan, Bull. Amer. Phys. Soc. **45**, 699 (2000).

14. C. A. Murray and D. H. Van Winkle, Phys. Rev. Lett. **58**, 1200 (1987).

15. K. Zahn, R. Lenke, and G. Marett, Phys. Rev. Lett. **82**, 2721 (1999).

16. J. Ruiz-Garcia, R. Gamez-Corrales, and B. I. Ivlev, Physica A **236**, 97 (1997).

17. J. Ruiz-Garcia, R. Gamez-Corrales, and B. I. Ivlev, Phys. Rev. E **58**, 660 (1998).

18. J. Ruiz-Garcia and B. I. Ivlev, Mol. Phys. **95**, 37 (1998).

19. T. Chou and D. R. Nelson, Phys. Rev. E **48**, 4611 (1993).

20. J. Rubi and J. M. G. Vilar, J. Phys.: Condens. Matter **12**, A75 (2000).

21. E. B. Sirota, H. D. Ou-Yang, S. K. Sinha, P. M. Chaikin, P. Pincus, J. D. Axe, and Y. Fujii, Phys. Rev. Lett. **62**, 1524 (1989).

22. H. Lowen, P. A. Madden, and J.-P. Hansen, Phys. Rev. E **68**, 1081 (1992).

23. M. Ospeck and S. Fraden, J. Chem. Phys. **109**, 9166 (1998).

24. G. M. Kepler and S. Fraden, Phys. Rev. Lett. **73**, 356 (1994).

25. J. C. Crocker and D. G. Grier, Phys. Rev. Lett. **77**, 1897 (1996).

26. D. G. Grier, Nature **393**, 621 (1998).

27. A. E. Larsen and D. G. Grier, Nature **385**, 230 (1997).

28. T. M. Squires and M. P. Brenner, Phys. Rev. Lett. **85**, 4976 (2000).

29. V. Lobaskin, M. Brunner, C. Bechinger, and H. H. von Grünberg, J. Phys.: Condens. Matter **15**, 6693 (2003).

30. C. Bechinger, private commun. (2005).

31. M. Gyger, *Master Thesis*, Universität Leipzig (2006).

32. I. E. Dzyaloshinskii, E. M. Lifshitz, and L. P. Pitaevskii, Adv. Phys. **10**, 165 (1961).

33. B. I. Ivlev, J. Phys.: Condens. Matter **14**, 4829 (2002).

34. L. D. Landau and E. M. Lifshitz, *Fluid Mechanics*, Butterworth-Heinemann (1997).

35. D. Drosdoff and A. Widom, Phys. Rev. E **73**, 051402 (2006).

36. J. Mahanty and B. W. Ninham, *Dispersion Forces*, Acad. Press, London (1976).

37. G. Barton, *Elements of Green's Functions and Propagation*, Claredon Press, Oxford (1989).